

Stabilization of the resistive wall mode instability by trapped energetic particles

G. Z. Hao, Y. Q. Liu, A. K. Wang, H. B. Jiang, Gaimin Lu et al.

Citation: *Phys. Plasmas* **18**, 032513 (2011); doi: 10.1063/1.3569854

View online: <http://dx.doi.org/10.1063/1.3569854>

View Table of Contents: <http://pop.aip.org/resource/1/PHPAEN/v18/i3>

Published by the [American Institute of Physics](#).

Related Articles

Collision frequency dependence of polarization current in neoclassical tearing modes

Phys. Plasmas **19**, 032120 (2012)

Effects of beam temperature and density variation on the growth rate of a two-stream free electron laser

Phys. Plasmas **19**, 032114 (2012)

The limits and challenges of error field correction for ITER

Phys. Plasmas **19**, 056111 (2012)

Dynamic contraction of the positive column of a self-sustained glow discharge in molecular gas

Phys. Plasmas **19**, 033512 (2012)

Wall-locking of kink modes in a line-tied screw pinch with a rotating wall

Phys. Plasmas **19**, 056104 (2012)

Additional information on Phys. Plasmas

Journal Homepage: <http://pop.aip.org/>

Journal Information: http://pop.aip.org/about/about_the_journal

Top downloads: http://pop.aip.org/features/most_downloaded

Information for Authors: <http://pop.aip.org/authors>

ADVERTISEMENT



HAVE YOU HEARD?

Employers hiring scientists
and engineers trust
physicstodayJOBS



<http://careers.physicstoday.org/post.cfm>

Stabilization of the resistive wall mode instability by trapped energetic particles

G. Z. Hao,^{1,a)} Y. Q. Liu,² A. K. Wang,¹ H. B. Jiang,¹ Gaimin Lu,¹ H. D. He,¹ and X. M. Qiu¹

¹Southwestern Institute of Physics, P.O. Box 432, Chengdu 610041, China

²Euratom/CCFE Fusion Association, Culham Science Centre, Abingdon, Oxon OX14 3DB, United Kingdom

(Received 26 January 2011; accepted 1 March 2011; published online 29 March 2011)

A theoretical model for investigating the effect of the trapped energetic particles (EPs) on the resistive wall mode (RWM) instability is proposed. The results demonstrate that the trapped EPs have a dramatic stabilizing effect on the RWM because of resonant interaction between the mode and the magnetic precession drift motion of the trapped EPs. The results also show that the effect of the trapped EPs depends on the wall position. In addition, the stabilizing effect becomes stronger when the plasma rotation is taken into account. For sufficiently fast plasma rotation, the trapped EPs can lead to the complete stabilization of the RWM. Furthermore, the trapped EPs can induce a finite real frequency of the RWM in the absence of plasma rotation. © 2011 American Institute of Physics. [doi:10.1063/1.3569854]

I. INTRODUCTION

One of the major goals of the magnetic confinement devices is to produce high- β (ratio of plasma to magnetic pressures) plasma at steady state. However, the maximum achievable β is often restricted by macroscopic magnetohydrodynamic (MHD) instabilities, such as the external kink mode. The latter can be completely stabilized by a perfectly conducting wall placed close enough to the plasma edge. However, in reality, the wall with finite conductivity will convert the fast-growing kink mode to the slowly growing resistive wall mode (RWM) at the time scale of the wall eddy current decay time. The RWM is unstable in the high β regime $\beta_N^{\text{no-wall}} < \beta_N < \beta_N^{\text{ideal}}$, where $\beta_N^{\text{no-wall}}$ and β_N^{ideal} are the so-called normalized β limits without and with an ideal wall, respectively, where β_N is defined as $\beta_N = \beta[\%]a[\text{m}]B[\text{T}]/I[\text{MA}]$ with a , I , and B being a plasma minor radius, current, and toroidal magnetic field, respectively.

Earlier theories¹⁻⁴ have shown that the unstable RWM can be fully suppressed by a combination of the plasma toroidal rotation and an energy dissipation mechanism. The critical plasma rotation needed for full stabilization of the mode depends on the choice of the damping model.⁵ It has been suggested that the critical plasma rotation frequency is a few percent of the Alfvén frequency at the $q=2$ rational surface.^{2,4} A strong viscous term modeling the Landau damping (sound wave resonance) was introduced into the MHD description,⁴ and possibly this term resulted in the critical rotation frequency comparable to the value of experimental observations.⁶⁻⁸

A damping model,⁹ including the kinetic contributions resulting from resonance of the mode with the bounce motion of thermal particles, has also been suggested. It was found that in some cases the predicted threshold value can be comparable to the experimental values.^{7,10-12} Recently, a kinetic damping model, including resonance between the mode

with the magnetic precession drifts of the trapped thermal particles, for the RWM instability was suggested.^{5,13,14} This kinetic damping can lead to full stabilization of the RWM in the plasmas with very slow rotation or even without one. Ref. 15 found that the kinetic contribution of fusion born α particles generally led to better stabilization compared with the thermal particle kinetic contribution alone. Ref. 16 suggested that the stabilization of the EPs on the RWM is roughly proportional to the ratio of the trapped EPs beta to the plasma pressure, but nearly independent on the plasma rotation. Ref. 17 showed that a new instability with small growth rate can be excited when the trapped EPs were taken into account in the RWM dispersion relation. However, the effect of the trapped EPs on the RWM has not been fully resolved, and could be crucial for the future tokamak devices.¹⁸

The present paper focuses on the stabilization of the trapped EPs on the RWM instability. In Refs. 15 and 16, the kinetic contribution from the mode-particle resonance to the RWM dispersion relation was evaluated numerically. In contrast, this work presents the analytic formulation to express the perturbed energies terms in the extended RWM dispersion relation. It should be pointed out that this work neglects the finite orbit width (FOW) of the EPs. Normally the FOW effect tends to reduce the stabilizing effect.¹⁴ Therefore, in reality, we expect that the stabilizing effect on the RWM might be weaker than this theory prediction.

The dispersion relation of the RWM taking the trapped EPs into account are carried out in Sec. II. In Sec. III, the numerical results of the dispersion relation are presented and discussed in detail. Finally, Sec. IV is the conclusions and discussion.

II. DISPERSION RELATION

The extended dispersion relation of the RWM with the contribution of the trapped EPs, is obtained as^{5,19}

^{a)}Electronic mail: haogz@swip.ac.cn.

$$D \equiv -i\omega\tau_w^* + \frac{\delta W^\infty + \delta W_{K0}}{\delta W^b + \delta W_{K0}} = 0, \quad (1)$$

where $\omega = \omega_r + i\gamma$ is the eigenvalue of the RWM. $\tau_w^* = \mu_0 \sigma b d (1 - a^{2m}/b^{2m})/m$ is defined as the typical wall eddy current decay time, with a , b , d , σ , m , and μ_0 being the plasma minor radius, the wall minor radius, the wall thickness, the wall conductivity, the poloidal mode number, and the permeability of free space, respectively. δW^∞ and δW^b express the perturbed fluid energies without and with an ideal wall, respectively, where the fluid energy includes the contributions from both the plasma and vacuum. δW_{K0} denotes the perturbed energy induced by the trapped EPs, which can be considered as the counterpart of the perturbed fluid energy of the plasma. Here, δW_{K0} consists of the kinetic component δW_k and fluid component $\delta W_{\text{MHD},h}$ written as the following formulations, respectively,

$$\delta W_k = -2^{9/2} \pi^3 R m_h \int Br dr \int d\alpha \int dE E^{5/2} K_b \bar{J}^* \times \frac{Q}{\omega - \omega_0 - \omega_d} \bar{J}, \quad (2)$$

$$\delta W_{\text{MHD},h} = - \int d^3x (\xi_\perp \cdot \nabla P_{h\perp}) (\xi_\perp^* \cdot \kappa), \quad (3)$$

where the variables ξ_\perp , $\kappa = (\mathbf{b} \cdot \nabla) \mathbf{b}$, $P_{h\perp}$, and m_h represent the perpendicular plasma displacement, magnetic curvature, perpendicular EPs pressure, and EP mass, respectively; r and R are the radial variable and major radius of the torus, respectively; $B = B_0(1 - \epsilon \cos \theta)$ denotes the equilibrium magnetic field to the lowest order in $\epsilon = r/R$, with θ being the poloidal angle; $J = (\alpha B/2 - 1) \xi_\perp \cdot \kappa$ with $\alpha = \mu m_h / E_k$ ($\mu = v_\perp^2 / 2B$ and $E_k = m_h v^2 / 2 \equiv m_h E$ are the magnetic moment and the kinetic energy of EPs, respectively); $Q = (\omega - \omega_0) \partial F / \partial E - (\partial F / \partial r) / (r \omega_c)$ with F and ω_c being the distribution function, cyclotron frequency of the trapped EPs, respectively; K_b is defined as $K_b = \int_{-\theta_b}^{\theta_b} (1 - \alpha B)^{-1/2} d\theta / \pi = 2\sqrt{2} / (\epsilon \alpha B_0) K(k_t) / \pi$, with θ_b being the turning point of the trapped EP. Here, we have used \bar{J} to denote the bounce-average of J (\bar{J}^* is the complex conjugate of \bar{J}); ω_d has been used to express the bounce-average toroidal drift precession frequency of the trapped EPs, $\omega_d = K_2 E q / (K_b r \omega_c R)$, with q being the safety factor and $K_2 = \int_{-\theta_b}^{\theta_b} (1 - \alpha B)^{-1/2} \cos \theta d\theta / \pi = 2\sqrt{2} / (\epsilon \alpha B_0) [2E(k_t) - K(k_t)] / \pi$, where $K(k_t)$ and $E(k_t)$ are the complete elliptic integrals of the first and second kinds, respectively, with the argument $k_t = (1/\alpha B_0 + \epsilon - 1) / (2\epsilon)$ [in the following, $E(k_t) \equiv E$ and $K(k_t) \equiv K$]. αB_0 is defined as the pitch angle of the trapped EPs. In addition, we have used ω_0 to denote the plasma rotation frequency (i.e., Doppler shift frequency), which is actually the toroidal component of the $\mathbf{E} \times \mathbf{B}$ flow in the plasma with \mathbf{E} being the total electric field in the tokamak devices. Hence, the direction of the ω_0 is determined by the direction of \mathbf{E} . From Eq. (2), we can see that the mode-particle resonance condition occurs at $\omega_r - \omega_d - \omega_0 = 0$, where the precession frequency ω_d depends on both the EPs energy and the minor radius r .

We notice that analytic work has been made for the double-kink mode ($m=2$, $n=1$).^{20,21} However, the above cited work investigated the destabilization of trapped EPs on the double-kink mode with a special choice of the top-hat structure for the mode eigenfunction. In this work, for simplicity, we choose the external kink mode eigenfunction for a cylindrical equilibrium¹⁹ to calculate the toroidal quantities δW_{K0} and $\delta W_{\text{MHD},h}$. Following Ref. 19, the perpendicular displacement of the instability is taken as $\xi_\perp = a m \hat{r}^{m-1} (\mathbf{e}_r + i \mathbf{e}_\theta) e^{i(m\theta - n\phi)} / F_0$ with n being the toroidal mode number, $F_0 = (m - nq)a / (Rq)$ and $\hat{r} = r/a$. From these, the quantity \bar{J} can be obtained as $\bar{J} = (1 - \alpha B_0/2) e^{i(-n\phi)} K_2 m a \hat{r}^{m-1} / (2RF_0 K_b)$. Here, we consider the case $m=2$, $n=1$. The perpendicular beta of the trapped EPs, averaged over the plasma volume, is given as

$$\beta_h = \left[\int d^3x (P_{h\perp}) / (B^2/2\mu_0) \right] / V = c_\beta \int r dr d\alpha dE K_b E f, \quad (4)$$

where $c_\beta = \pi N_p \mu_0 m_h / (R B a^2)$ and $P_{h\perp} = m_h \int d^3v E F$; $f = 2^{5/2} R \sqrt{E F} / N_p$ is the normalized distribution function of the EPs with N_p being the total number of the EPs. In the following analytical derivation, all of the energies are normalized to $\pi B^2 a^4 m^2 / (2R \mu_0 F_0^2)$.

On the basis of Eqs. (2)–(4), the contribution of the trapped EPs to the RWM dispersion relation can be obtained as

$$\begin{aligned} \delta W_{K0} &= \delta W_k + \delta W_{\text{MHD},h} \\ &= 12\pi \left(1 - \frac{\alpha_0 B_0}{2}\right)^2 \frac{\beta_h R}{K a} \left\{ (\hat{A} - \hat{B}) \frac{2}{7} \Omega \ln \left(1 - \frac{1}{\Omega}\right) \right. \\ &\quad - \frac{2}{7} \left(\hat{A} + \frac{5}{2} \hat{B}\right) \Omega \left[2 \left(\frac{1}{5\Omega} + \frac{1}{3\Omega^2} + \frac{1}{\Omega^3}\right) \right. \\ &\quad \left. \left. - \frac{1}{\Omega^3} \frac{1}{\sqrt{\Omega}} \ln \left(\frac{1 + \sqrt{\Omega}}{1 - \sqrt{\Omega}}\right) \right] \right\} + M, \end{aligned} \quad (5)$$

where $\Omega \equiv i\Gamma \omega_A / \omega_{ds} + \Omega_r - \Omega_0$,

$$\begin{aligned} \hat{A} &= \frac{1}{q} (2m - 2)(2E - K) \\ &\quad + \left(1 - \frac{1}{q}\right) \left[(1 - 2k_t) K \frac{d}{dk_t} \left(\frac{E}{K}\right) - (2E - K) \right] \\ &\quad + \frac{1}{2} (2E - K) - \frac{1}{\alpha_0 B_0} (2E - K) \frac{d}{dk_t} \left(\frac{E}{K}\right) - \left[\frac{1}{\alpha_0 B_0} \frac{E}{K} \right. \\ &\quad \left. + k_t - \frac{1}{2\alpha_0 B_0} - \frac{1}{2} \right] \frac{d}{dk_t} (2E - K), \end{aligned} \quad (6)$$

$$\hat{B} = \left[\frac{1 - 2k_t}{q} - \frac{1}{\alpha_0 B_0} \left(2\frac{E}{K} - 1\right) \right] K \frac{d}{dk_t} \left(\frac{E}{K}\right) - \frac{(2E - K)}{q}, \quad (7)$$

$$M = -\beta_h \frac{3\pi R}{2Ka} \frac{1-2k_t}{2m-3/2} \left[\frac{q-4(1-0.5\alpha_0 B_0)^2}{q} \right] \times \frac{d}{dk_t} (2E-K), \quad (8)$$

where $\Gamma = \gamma/\omega_A$, $\Omega_r = \omega_r/\omega_{ds}$, and $\Omega_0 = \omega_0/\omega_{ds}$ denote the normalized RWM growth rate, RWM real frequency and plasma rotation frequency, respectively. We have used $\omega_A = B_0/(R\sqrt{\mu_0\rho})$ to express the Alfvén frequency with ρ being the plasma mass density; $\omega_{ds} = K_2(a)E_m q/[K_b(a)a\omega_c R]$ has been used to denote the precession drift frequency of the trapped EPs at the plasma edge with $m_h E_m (=E_b)$ being the birth energy of the trapped EPs. The choice of different normalizations for the mode growth rate and the mode frequency is motivated by the convenience of physical interpretation of the results. While the Alfvén frequency is one of the convenient choices for measuring the physical growth of the mode, the normalization of Ω_r and Ω_0 , by the EPs precession frequency (at birth energy), better reflects the resonant conditions in our context. Furthermore, if $q=1$ and $m=1$ are assumed, the formulas \hat{A} and \hat{B} can recover to those given in Ref. 22 and M is equal to zero at the same time. In order to obtain a simple expression of δW_{K0} , we have assumed that the argument k_t are not functions of r and α , being approximately replaced by the edge value. This approximation, also adopted in Ref. 22, seems to be reasonable. As a consequence, \hat{A} and \hat{B} become constants and M becomes a constant multiplied by β_h . In addition, we also assume an anisotropic slowing-down equilibrium distribution function $F = n_t \delta(\alpha_0 - \alpha) E^{-3/2}$ for the EPs induced by neutral beam injection. The corresponding f is written as $f = n_0 \delta(\alpha - \alpha_0) E^{-1}$ with $n_0 = 2^{5/2} R n_t / N_p$. In Eq. (5), the imaginary part of the kinetic contribution δW_{K0} [denoted by $\text{Im}(\delta W_{K0})$] will significantly affect the growth rate and real frequency of the RWM.

The normalized forms of the fluid potential energy without and with an ideal wall are given,¹⁹ respectively, as

$$\delta W^\infty = \frac{-4\pi(m-nq)^2}{m} \frac{1}{q^2} \left(\frac{1}{m-nq} - 1 \right) \quad (9)$$

and

$$\delta W^b = \frac{-4\pi(m-nq)^2}{m} \frac{1}{q^2} \left(\frac{1}{m-nq} - \frac{1}{1-b^{-2m}} \right), \quad (10)$$

where b is normalized to the plasma minor radius a . Submitting Eqs. (5), (9), and (10) into Eq. (1), we can obtain the normalized dispersion relation

$$D \equiv -i(\Omega_r + i\Gamma\omega_A/\omega_{ds})\omega_{ds}\tau_w^* + \frac{\delta W^\infty + \delta W_{K0}}{\delta W^b + \delta W_{K0}} = 0. \quad (11)$$

When the effect of trapped EPs is taken into account, the eigenvalue of the RWM should be modified according to Eq. (11). The numerical results are presented in the next section. It is worthwhile to note that the inclusion of the eigenvalue in δW_{K0} makes the eventual eigenvalue problem nonlinear, allowing the existence of multiple roots for Eq. (11). However, in this work, we only focus on the RWM branch, whose

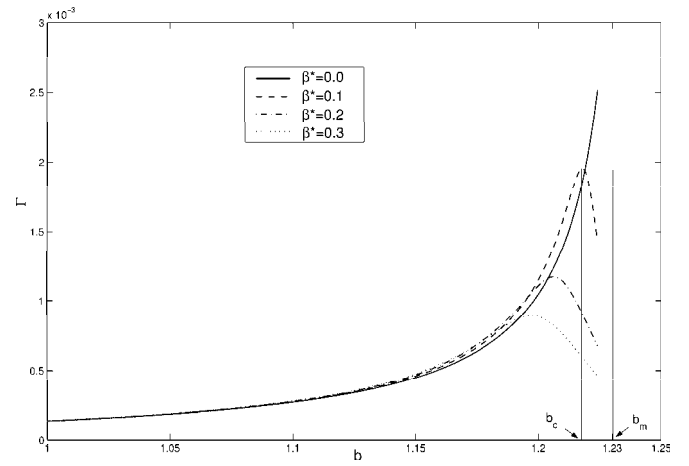


FIG. 1. The RWM growth rate Γ (normalized to ω_A) vs the wall minor radius b for the different values of β^* ($\equiv \beta_h/\beta$). Here, b_c is the wall position at which the value of Γ achieves its maximum value. No plasma rotation is assumed.

growth rate traces back to the fluid case at vanishing kinetic effect from the trapped EPs. In addition, it should be noted that δW_{K0} is calculated for a large aspect ratio toroidal plasma, while δW^∞ and δW^b are evaluated for a cylindrical plasma. Nevertheless, we expect that the toroidal corrections to the fluid potential energies, and the cylindrical external kink mode eigenfunction used for calculating δW_{K0} , do not alter the qualitative conclusions of this work.

In Eq. (11), without kinetic effects, $\delta W^\infty < 0$ and $\delta W^b > 0$ imply that the RWM is unstable without ideal wall and stable with an ideal wall placed at b , respectively. In other words, the opposite signs of δW^∞ and δW^b indicate that the plasma is in the regime of wall-stabilized ideal external kink and unstable RWM. Moreover, $\delta W^b > 0$ leads to a constraint condition on the wall position $b < b_m \equiv [1/(nq-m+1)]^{1/2m}$ in this work, where b_m is defined as the ideal-wall marginal position. In addition, the expression of δW^b in Eq. (10) shows that the value of δW^b decreases with increasing b , and the value of δW^b recovers to that of δW^∞ if we set $b \rightarrow \infty$.

III. NUMERICAL RESULTS AND DISCUSSIONS

In the following calculations, the parameters are chosen as: $m=2$, $n=1$, $a=1$ m, $R=3$ m, $B_0=2.3$ T, $E_b=85$ KeV, $q=1.42$, $\beta=0.055$, $\sigma=10^6$ Ω^{-1} m⁻¹, $d=0.01a$, $\alpha_0 B_0=0.98$, and the density $n_0=10^{20}$ m⁻³. The choice of the harmonic numbers and the (flat) q value yields an RWM regime (i.e., $\delta W^\infty < 0$ and $\delta W^b > 0$). The choice of the wall characteristics gives typical RWM growth rates. The other parameters correspond to a conventional tokamak plasma, with the neutral beam induced energetic ions. For the parameters chosen above, the following values can be obtained $\omega_{ds}=7.3 \times 10^3$ s⁻¹, $\omega_A=1.7 \times 10^6$ s⁻¹, and $b_m=1.23$. Here, for the definition of the Alfvén frequency, we use the ion mass for hydrogen ion instead of that for deuterium ion. However, this definition would not change the qualitative conclusion in our work.

Figure 1 plots the normalized growth rate Γ with varying the wall position b for various values of β^* ($\equiv \beta_h/\beta$) in the

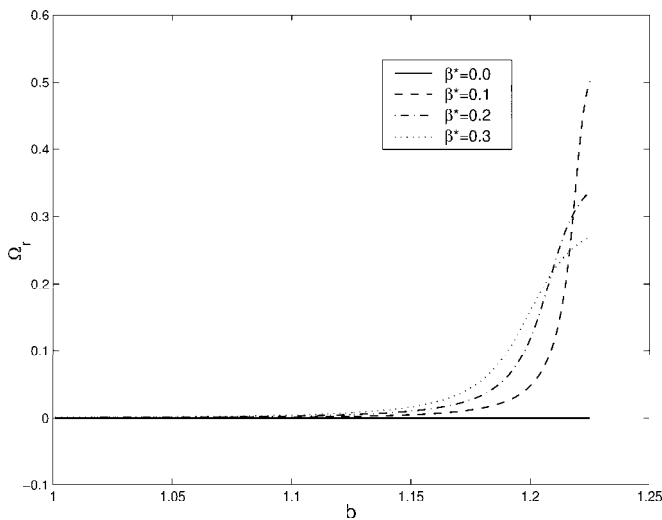


FIG. 2. The RWM frequency Ω_r (normalized to ω_{ds}) as a function of the wall minor radius b for the different values of β^* , where ω_{ds} expresses the precession drift frequency of the trapped EPs with the birth energy at the plasma edge. No plasma rotation is assumed.

absence of the plasma rotation (i.e., $\Omega_0=0$). Here, the maximum of β^* is in the order of a/R .^{22,23} Figure 1 indicates that the value of Γ monotonically increases with position b for the case without trapped EPs contribution (i.e., $\beta^*=0$). However, for the cases of $\beta^*=0.1$, $\beta^*=0.2$ and $\beta^*=0.3$, the Γ increases with increasing b initially, and then decreases gradually after reaching a maximum at certain value b_c which is inversely proportional to β^* . It also shows that the stabilization of trapped EPs on the mode is strong when the wall is placed in the region $b > b_c$. In other words, the stabilization becomes strong when the wall approaches the ideal-wall marginal point $b_m (=1.23)$. The reason for kinetic stabilizing effect appearing near the ideal-wall marginal point, is mainly due to the fact that the denominator in Eq. (11) is easily modified by the kinetic contribution when δW_b approaches zero. The stabilization mechanism is due to the energy dissipation resulting from the resonance between the EP-induced finite mode frequency ($\Omega_r - \Omega_0$) and the EP's precession drift frequency ($\Omega_d = \omega_d / \omega_{ds}$), that is satisfied for EPs at particular radial locations and with particular energy. It is worthy to point out that the condition either $\Omega_d < 1$ (i.e., $\omega_d < \omega_{ds}$) or $\Omega_d > 1$ (i.e., $\omega_d > \omega_{ds}$) is possible, due to the fact that the true ω_d is dependent on the EPs energy and the minor radius r while ω_{ds} is kept constant in this paper, as mentioned in Sec. II.

Figure 2 plots the real frequency of the RWM Ω_r as functions of b for the cases of $\beta^*=0.0$, $\beta^*=0.1$, $\beta^*=0.2$, and $\beta^*=0.3$. As expected, Fig. 2 shows that for the case of $\beta^*=0.0$, the mode frequency Ω_r is equal to zero for all b values. This is due to that the RWM dispersion relation for the static plasma with $\beta^*=0.0$ is determined by $D \equiv -i\omega\tau_w^* + \delta W^\infty / \delta W^b = 0$ with neglecting the contributions from both the plasma inertial term and the dissipation term.²⁴ For the static fluid RWM, the fluid potential energies both δW^∞ and δW^b are real numbers, which determine that the RWM just has the growth rate (i.e., $\omega = i\gamma$). However, when the trapped EPs effects are included, the RWM eigenvalue can be sig-

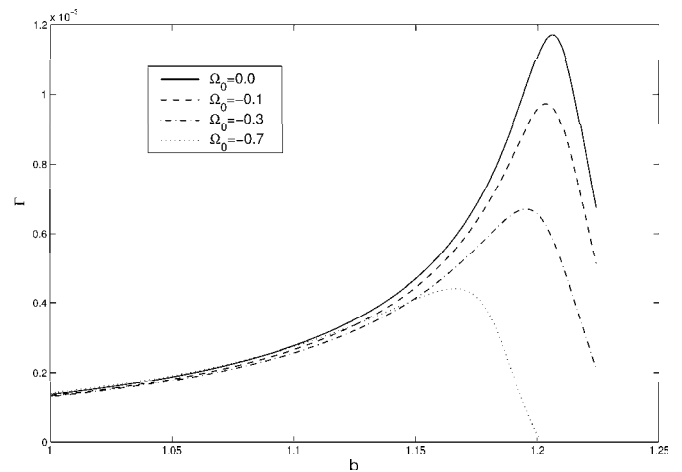


FIG. 3. The dependence of the RWM growth rate Γ on the wall minor radius b for the different values of $\Omega_0 (\equiv \omega_0 / \omega_{ds})$, where ω_0 denotes the plasma rotation frequency (i.e., Doppler shift frequency). The value of β^* is taken as 0.2.

nificantly influenced the kinetic term δW_{K0} which can be a complex quantity. As well known, $\text{Im}(\delta W_{K0})$ always mitigates the RWM growth rate.⁵ But, the real part $\text{Re}(\delta W_{K0})$ can either stabilize the RWM or destabilize it, which depends on the specific system parameters. In addition, the term $\text{Im}(\delta W_{K0})$ can also induce the finite real frequency of the RWM even in the ideal plasma without the plasma rotation. Here, it is worthy to notice that the imaginary part of the dispersion relation Eq. (11) can be written as

$$\begin{aligned} \text{Im}(D) &\equiv \Omega_r \omega_{ds} \tau_w^* - \frac{(\delta W^b - \delta W^\infty) \text{Im}(\delta W_{K0})}{\{[\delta W^b + \text{Re}(\delta W_{K0})]^2 + \text{Im}(\delta W_{K0})^2\}} \\ &= 0. \end{aligned} \quad (12)$$

From the above formula, it can be clearly seen that the term $\text{Im}(\delta W_{K0})$ results in the mode real frequency and $|\text{Re}(\delta W_{K0})|$ could significantly modify the real frequency magnitude when $|\text{Re}(\delta W_{K0})|$ is comparable to δW^b . Generally, in the framework of the MHD description theory, the real frequency of the mode is induced by the plasma rotation or some viscosities such as the parallel viscosity or the turbulent viscosity.²⁵

From Fig. 2, we also see that the Ω_r is approximately proportional to b for the cases of $\beta^*=0.1$, $\beta^*=0.2$, and $\beta^*=0.3$. In addition, it is shown the kinetic modification of the trapped EPs on the mode real frequency becomes significant near the ideal-wall marginal point b_m . These computations indicate that when the effects of the trapped EPs are taken into account, the RWM possesses dramatic real frequency Ω_r near the b_m in the absence of the plasma rotation and the direction of the Ω_r is the same with that of the precession drift of trapped EPs. From Figs. 1 and 2, we can note that the kinetic modification can significantly modify the RWM eigenvalue near the b_m , but hardly give contributions to the mode eigenvalue when the wall is placed near the plasma edge.

Figure 3 displays the RWM growth rate Γ as functions of the wall position b for different choices of the plasma rotation Ω_0 , while the $\beta^*=0.2$ is kept constant. Here, the

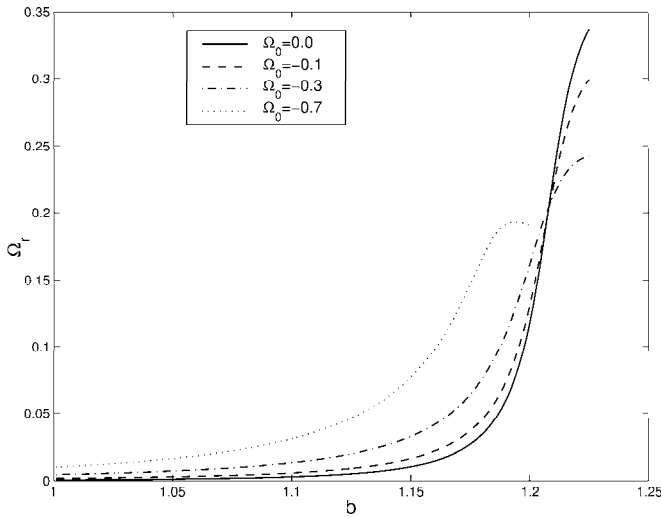


FIG. 4. The RWM real frequency Ω_r , as a function of the wall minor radius b for the different values of Ω_0 . The trapped EPs beta is chosen as $\beta^* = 0.2$.

minus sign of Ω_0 implies that the direction of the plasma rotation is opposite to that of the trapped EPs precession drift motion. In our case, the negative Ω_0 leads to an enhanced mode-particle resonance interaction, while the positive Ω_0 should lead to a reduced resonance (i.e., a destabilization compared to the zero rotation case). We can see that the achievable maximum of Γ along the wall position is inversely proportional to the value of $|\Omega_0|$. That is, the plasma rotation can enhance stabilization of trapped EPs on the RWM growth rate. It can also be confirmed by the fact that the appearance of Ω_0 can increase the value of $\text{Im}(\delta W_{K0})$ which can result in the mitigation of the RWM growth rate (see Fig. 7, for more details). Hence, the stabilization of trapped EPs on the mode growth rate depends on the plasma rotation. On the other hand, the value of b_c decreases with increasing $|\Omega_0|$. For instance, the value of b_c for the case of $\Omega_0 = -0.7$ is smaller than that corresponding to $\Omega_0 = -0.1$ as shown in Fig. 3. Furthermore, Fig. 4 displays the curves of Ω_r versus b in the presence of plasma rotation. It is worthy to note that at $b \approx 1$, the mode possesses a finite real frequency for the cases with finite plasma rotation and the value of Ω_r is slightly proportional to $|\Omega_0|$. It implies that the effect of Ω_0 on the mode real frequency is “global” from the plasma edge to the wall position.

In order to investigate the dependence of the b_c on the quantities Ω_0 and β^* in detail, Fig. 5 shows the b_c diagram in the $\beta^* - \Omega_0$ plane. In Fig. 5, the solid, dashed and dot-dashed curves correspond to $b_c = 1.15$, $b_c = 1.18$, and $b_c = 1.2$, respectively. It clearly indicates that both the β^* and the Ω_0 can reduce the value of b_c .

Figure 6 shows the dependence of the mode growth rate Γ on the trapped EPs beta β^* for different choices of the plasma rotation Ω_0 with the fixed wall position $b = 1.2$. For the parameters given above, we can obtain $\tau_w^*/\tau_A = 3.6 \times 10^3$, where $\tau_A = 1/\omega_A$. In addition, δW^b and δW^∞ are equal to 0.22 and -0.76 , respectively. For a specific choice of $\Omega_0 (= -0.7)$ in Fig. 6, increasing the trapped EPs β^* , the mode is initially slightly destabilized at lower β^* , followed by the significant stabilization at higher β^* . Furthermore, the comparison be-

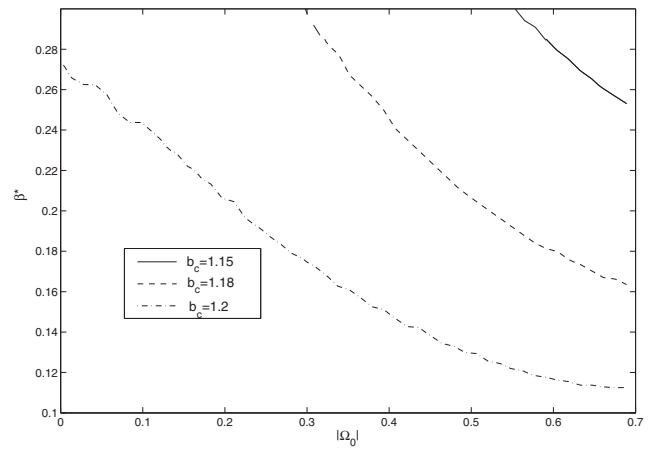


FIG. 5. The b_c diagram in the $\beta^* - \Omega_0$ plane. The different styles of the curves denote the different choices of b_c .

tween the different curves shows that the stabilizing effect becomes more substantial as the plasma rotation increases. It is shown that for the case of $\Omega_0 = -0.7$, the mode can be fully suppressed (i.e., $\Gamma = 0$) when β^* is equal to about 0.21. Therefore, the plasma finite rotation frequency is crucial for the trapped EPs to fully stabilize the RWM. Here, $\Omega_0 = -0.7$ is equivalent to $|\omega_0|/\omega_A = 0.3\%$. This value of the plasma rotation is possible to be sustained for the further advanced tokamaks.¹² Furthermore, if other stabilization mechanisms, such as the strong stabilization of the trapped thermal particles and the typical continuum damping resulted from Alfvén and sound waves, are considered at the same time, the rotation frequency required for the RWM full suppression can be slower or even approaches to zero. Similar to discussions proposed in Ref. 5, we can expect that the trapped energetic electrons can also reduce the RWM growth rate, if the plasma rotation magnitude and its direction are chosen appropriately.

Based on Eq. (11), we obtain $\Gamma \omega_A \tau_w^* = (\delta W^b - \delta W^\infty) \times [\delta W^b + \text{Re}(\delta W_{K0})] / \{[\delta W^b + \text{Re}(\delta W_{K0})]^2 + \text{Im}(\delta W_{K0})^2\} - 1$.

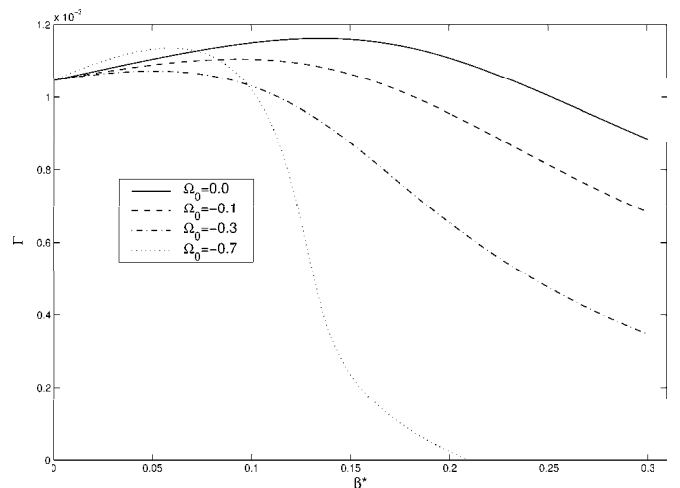


FIG. 6. The RWM normalized growth rate Γ as functions of the EPs beta β^* for various values of the plasma rotation frequency Ω_0 . The wall position is taken as $b = 1.2$.

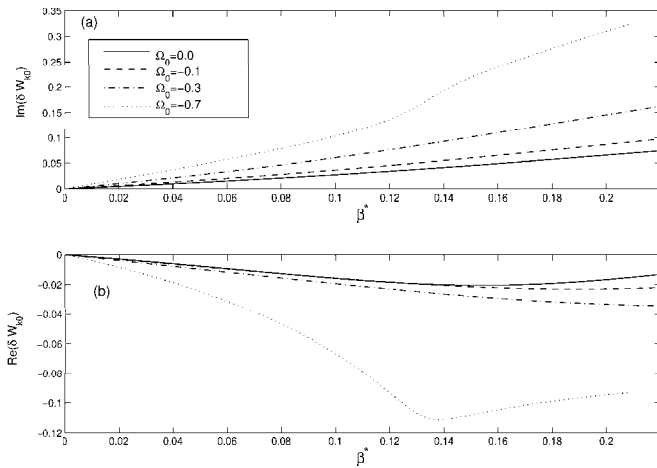


FIG. 7. Imaginary part $\text{Im}(\delta W_{K0})$ and the real part $\text{Re}(\delta W_{K0})$ of the perturbed energy of the trapped EPs vs the trapped EPs beta β^* for the different choices of the plasma rotation frequency Ω_0 . The wall position is taken as $b=1.2$.

From the above equation, it can be seen that when $|\text{Im}(\delta W_{K0})| \gg |\delta W^b + \text{Re}(\delta W_{K0})|$, the Γ is inversely proportional to the value of $|\text{Im}(\delta W_{K0})|$. On the other hand, if $|\text{Im}(\delta W_{K0})| \ll |\delta W^b + \text{Re}(\delta W_{K0})|$, the effect of $\text{Re}(\delta W_{K0})$ on Γ becomes significant.

Figures 7(a) and 7(b) show the values of $\text{Im}(\delta W_{K0})$ and $\text{Re}(\delta W_{K0})$ as functions β^* for the different choices of Ω_0 , respectively. Figure 7(a) displays that the magnitude of $\text{Im}(\delta W_{K0})$ is proportional to β^* monotonically for a specific choice of Ω_0 . It also shows that the value of $|\text{Im}(\delta W_{K0})|$ corresponding to $\Omega_0 = -0.7$ is larger than that corresponding to $\Omega_0 = -0.1$ for a specific value of β^* . Therefore, the inclusion of Ω_0 can enhance the value of $|\text{Im}(\delta W_{K0})|$ to lead to the more mitigation of the RWM growth rate. Figure 7(b) shows that the value of $|\text{Re}(\delta W_{K0})|$ is nearly monotonically proportional to β^* for a case with smaller Ω_0 . Otherwise, for the case of $\Omega_0 = -0.7$, the $|\text{Re}(\delta W_{K0})|$ increases with β^* first, and then decreases gradually after reaching a maximum. It means that the dependence of $|\text{Re}(\delta W_{K0})|$ on β^* is related to the magnitude of the plasma rotation. When the plasma rotation is fast, the dependence of $|\text{Re}(\delta W_{K0})|$ on β^* is not monotonic any more. It is worthy to notice that at lower β^* , the condition $|\text{Im}(\delta W_{K0})| \ll |\delta W^b + \text{Re}(\delta W_{K0})|$ can be satisfied, and then the Γ is mainly determined by $\text{Re}(\delta W_{K0})$. Here, the negative value of $\text{Re}(\delta W_{K0})$ can result in the destabilization of the RWM by EPs at lower β^* , as shown in Fig. 6. On the other hand, at higher β^* for the case of $\Omega_0 = -0.7$, the relation $|\text{Im}(\delta W_{K0})| \gg |\delta W^b + \text{Re}(\delta W_{K0})|$ can be assumed, then the Γ mainly determined by the value of $|\text{Im}(\delta W_{K0})|$ is inversely proportional to β^* , as shown in Fig. 6.

Figure 8 shows the curves of Ω_r versus β^* for the various values of Ω_0 . For the cases of $\Omega_0 = 0.0$, $\Omega_0 = -0.1$, and $\Omega_0 = -0.3$, the Ω_r is roughly proportional to β^* , which is mainly due to that the value of $|\text{Re}(\delta W_{K0})|$ is much smaller than the that of δW^b and the magnitude of the Ω_r is principally determined by the value of $|\text{Im}(\delta W_{K0})|$. However, for the case with fast plasma rotation $\Omega_0 = -0.7$, $|\text{Re}(\delta W_{K0})|$ can be comparable to $\delta W^b (=0.22)$ when the β^* is large enough as

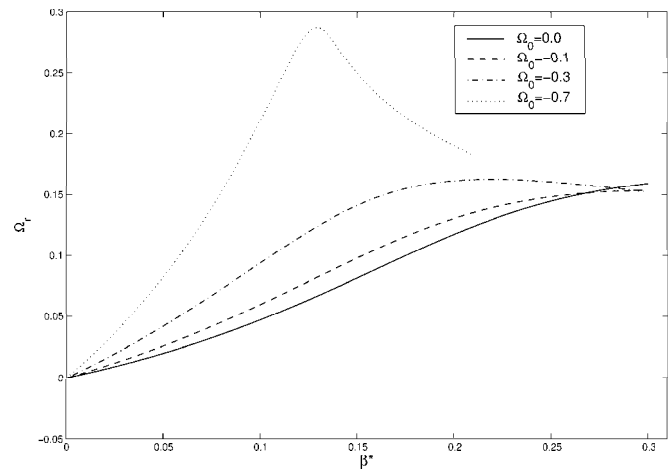


FIG. 8. The normalized real frequency Ω_r of the RWM as functions of the EPs beta β^* for various values of Ω_0 . The wall position is taken as $b=1.2$.

shown in Fig. 7(b). Then, $|\text{Re}(\delta W_{K0})|$ can significantly modify the real frequency of the RWM. Therefore, the dependence of Ω_r on the β^* is similar to that of $|\text{Re}(\delta W_{K0})|$ on the β^* for the case of $\Omega_0 = -0.7$, as shown in Fig. 7(b).

Figure 9 scans the kinetically modified RWM growth rate Γ as a function of the plasma rotations for different choices of β^* . It is shown that the higher $|\Omega_0|$ generally leads to the more suppression of the trapped EPs on the RWM growth rate for a specific choice of β^* . That is, the stabilization effect of the trapped EPs on the RWM can be enhanced by fast plasma rotation frequency.

IV. CONCLUSIONS

We have extended the RWM dispersion relation in terms of perturbed energies to investigate the effect of the trapped EPs on the RWM instability. The calculations show that the trapped EPs have significant stabilization on the RWM in the case of zero plasma rotation. For the case without plasma

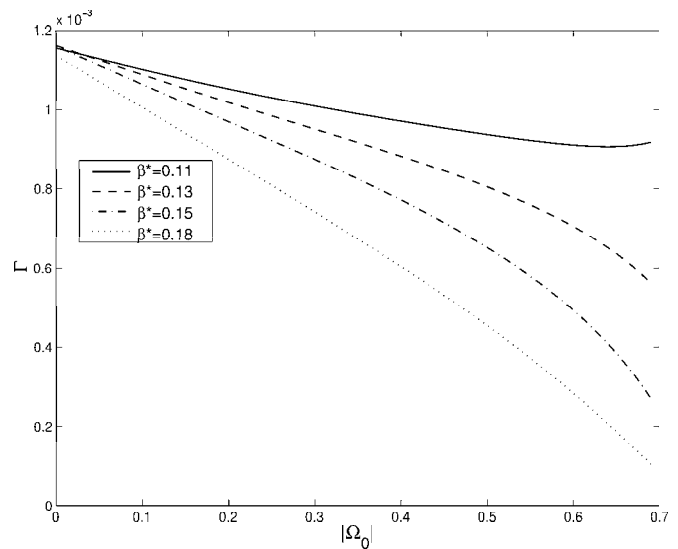


FIG. 9. The RWM growth rate Γ vs the plasma rotation frequency $|\Omega_0|$ for the different values of β^* . The wall position is taken as $b=1.2$.

rotation, the stabilization effect of trapped EPs on the RWM comes from the resonance between the EP-induced finite mode frequency with the EP's precession drift frequency. The stabilization is enhanced when the plasma rotation is taken into account. A complete stabilization can be achieved by the trapped EPs in the presence of the plasma rotation. This is due to the fact that the plasma rotation can lead to an enhanced mode-particle resonance interaction. In addition, the effect of trapped EPs on the RWM eigenvalue becomes weaker as the wall approaches to the plasma edge. The calculations also demonstrate that the real part of the perturbed energy of the trapped EPs $|\text{Re}(\delta W_{K0})|$ can significantly modify the real frequency of the RWM when it is comparable to δW^b . These conclusions are expected to be useful for the further understanding of the stability of the RWM in high-beta tokamak device and the interaction between the trapped EPs with the global MHD instability, or even for exploring the plasma response to the external electromagnetic fields. A more sophisticated model including, for example, the effects of the trapped thermal particles, the magnetic shear, and more realistic tokamak geometry, will be required in future work.

Finally, we compare our conclusions with that from previous numerical work.^{15,16} The agreement between our work with Refs. 15 and 16 is that EPs are generally stabilizing. The difference between our work with Ref. 16 is that we find stabilization mostly through the term $\text{Im}(\delta W_{K0})$, and it strongly depends on the plasma rotation frequency. Reference 16 finds that the major effect from EPs comes from $\text{Re}(\delta W_{K0})$, and the stabilization effect is not sensitive to rotation, due to the fact that the EP precession frequency is much larger than the plasma rotation frequency, in the rotation regime considered in Ref. 16. In our work, however, the rotation frequency does start to match the EP precession frequency and can give significant $\text{Im}(\delta W_{K0})$.

ACKNOWLEDGMENTS

The authors would like to thank the anonymous referee for constructive comments and suggestions. This work was supported by the National Natural Science Foundation of China under Grant No. 10775040 and also supported by National Magnetic Confinement Fusion Science Program under Grant No. 2009GB101002.

- ¹R. Fitzpatrick and A. Y. Aydemir, *Nucl. Fusion* **36**, 11 (1996).
- ²A. Bondeson and D. J. Ward, *Phys. Rev. Lett.* **72**, 2709 (1994).
- ³R. Betti and J. P. Freidberg, *Phys. Rev. Lett.* **74**, 2949 (1995).
- ⁴M. S. Chu, J. M. Greene, T. H. Jensen, R. L. Miller, A. Bondeson, R. W. Johnson, and M. E. Mauel, *Phys. Plasmas* **2**, 2236 (1995).
- ⁵B. Hu and R. Betti, *Phys. Rev. Lett.* **93**, 105002 (2004).
- ⁶R. J. La Haye, A. Bondeson, M. S. Chu, A. M. Garofalo, Y. Q. Liu, G. A. Navratil, M. Okabayashi, H. Reimerdes, and E. J. Strait, *Nucl. Fusion* **44**, 1197 (2004).
- ⁷Y. Liu, A. Bondeson, M. S. Chu, J.-Y. Favez, Y. Gribov, M. Gryaznevich, T. C. Hender, D. F. Howell, R. J. La Haye, J. B. Lister, P. de Vries, and EFDA JET Contributors, *Nucl. Fusion* **45**, 1131 (2005).
- ⁸Y. Liu, M. S. Chu, A. M. Garofalo, R. J. La Haye, Y. Gribov, M. Gryaznevich, T. C. Hender, D. F. Howell, P. de Vries, M. Okabayashi, S. D. Pinches, H. Reimerdes, and EFDA JET Contributors, *Phys. Plasmas* **13**, 056120 (2006).
- ⁹A. Bondeson and M. S. Chu, *Phys. Plasmas* **3**, 3013 (1996).
- ¹⁰Y. Q. Liu, A. Bondeson, C. M. Fransson, B. Lennartson, and C. Breitholtz, *Phys. Plasmas* **7**, 3681 (2000).
- ¹¹L. J. Zheng, M. T. Kotschenreuther, and J. W. Van Dam, *Nucl. Fusion* **49**, 075021 (2009).
- ¹²H. Reimerdes, A. M. Garofalo, G. L. Jackson, M. Okabayashi, E. J. Strait, M. S. Chu, Y. In, R. J. La Haye, M. J. Lanctot, Y. Q. Liu, G. A. Navratil, W. M. Solomon, H. Takahashi, and R. J. Groebner, *Phys. Rev. Lett.* **98**, 055001 (2007).
- ¹³B. Hu, R. Betti, and J. Manickam, *Phys. Plasmas* **12**, 057301 (2005).
- ¹⁴Y. Q. Liu, M. S. Chu, I. T. Chapman, and T. C. Hender, *Phys. Plasmas* **15**, 112503 (2008).
- ¹⁵Y. Q. Liu, *Nucl. Fusion* **50**, 095008 (2010).
- ¹⁶J. W. Berkery, S. A. Sabbagh, H. Reimerdes, R. Betti, B. Hu, R. E. Bell, S. P. Gerhardt, J. Manickam, and M. Podesta, *Phys. Plasmas* **17**, 082504 (2010).
- ¹⁷Y. Q. Liu, M. S. Chu, W. F. Guo, F. Villone, R. Albanese, G. Ambrosino, M. Baruzzo, T. Bolzonella, I. T. Chapman, A. M. Garofalo, C. G. Gimblett, R. J. Hastie, T. C. Hender, G. L. Jackson, R. J. La Haye, M. J. Lanctot, Y. In, G. Marchiori, M. Okabayashi, R. Paccagnella, M. Furno Palumbo, A. Pironti, H. Reimerdes, G. Rubinacci, A. Soppelsa, E. J. Strait, S. Ventre, and D. Yadykin, *Plasma Phys. Controlled Fusion* **52**, 104002 (2010).
- ¹⁸M. S. Chu and M. Okabayashi, *Plasma Phys. Controlled Fusion* **52**, 123001 (2010).
- ¹⁹Y. Q. Liu, M. S. Chu, C. G. Gimblett, and R. J. Hastie, *Phys. Plasmas* **15**, 092505 (2008).
- ²⁰C. G. Gimblett, R. J. Hastie, and T. C. Hender, *Phys. Plasmas* **3**, 3369 (1996).
- ²¹P. Helander, C. G. Gimblett, R. J. Hastie, and K. G. McClements, *Phys. Plasmas* **4**, 2181 (1997).
- ²²R. B. White, L. Chen, F. Romanelli, and R. Hay, *Phys. Fluids* **28**, 278 (1985).
- ²³L. Chen, R. B. White, and M. N. Rosenbluth, *Phys. Rev. Lett.* **52**, 1122 (1984).
- ²⁴S. W. Haney and J. P. Freidberg, *Phys. Fluid B* **1**, 1637 (1989).
- ²⁵G. Z. Hao, Y. Q. Liu, and A. K. Wang, *Proceedings of the 23rd IAEA Fusion Energy Conference* (International Atomic Energy Agency, Vienna, 2010), Paper No. THS/P5-07.